

## Article

# Preliminary Recognition of Geohazards at the Natural Reserve “Lachea Islet and Cyclop Rocks” (Southern Italy)

Giovanna Pappalardo <sup>1</sup>, Simone Mineo <sup>1,\*</sup>, Serafina Carbone <sup>1</sup>, Carmelo Monaco <sup>1,2,3</sup>, Domenico Catalano <sup>4</sup> and Giovanni Signorello <sup>4</sup>

<sup>1</sup> Department of Biological, Geological and Environmental Sciences, University of Catania, 95129 Catania, Italy; pappalar@unict.it (G.P.); carbone@unict.it (S.C.); cmonaco@unict.it (C.M.)

<sup>2</sup> CRUST—Interuniversity Center for 3D Seismotectonics with Territorial Applications, 66100 Chieti, Italy

<sup>3</sup> Istituto Nazionale di Geofisica e Vulcanologia, Osservatorio Etno, 95125 Catania, Italy

<sup>4</sup> CUTGANA Centro Universitario per la Tutela e la Gestione degli Ambienti Naturali e degli Agro-Ecosistemi, University of Catania, 95123 Catania, Italy; dcatalano@unict.it (D.C.); g.signorello@unict.it (G.S.)

\* Correspondence: smineo@unict.it

**Abstract:** In this study, we present a preliminary recognition of geohazards at the natural reserve archipelago “Lachea Islet and Cyclop Rocks” by integrating infrared thermography (IRT) and morphological-aerial interpretation. The study area, located in the wider setting of the UNESCO (United Nations Educational, Scientific and Cultural Organization) World Heritage Mount Etna (eastern Sicily), is a worldwide renowned tourist destination suffering from a limited fruition due to the instability of rock masses. The peculiar setting of the area, represented by steep sea rocks and an islet, requires the employment of remote surveying methodologies for the preliminary slope characterization in the perspective of safe ground surveys. In this paper, IRT analysis allowed the recognition of signs of past rockfalls, as well as the presence of loose rock material likely laying in unstable conditions, thanks to the variation of the surface temperature characterizing the slope. The combination of IRT outcomes with morphological-aerial data allowed recognizing the potential source areas of future rockfalls, which were modeled through trajectory simulations. Results showed that a relevant strip of sea surrounding the studied sea rock could be crossed by falling blocks, suggesting the need of instituting a forbidden area for a safe fruition of the reserve. Furthermore, IRT allowed for the recognition of some peculiar features linked to the presence of tectonic lines. Such correspondence was validated by a comparison with literature structural data, proving the potential of such remote methodological approach. This represents a new aspect of the application of IRT to other fields of geosciences, thus representing a starting point for the scientific development of new technological branches.

**Keywords:** geohazard; natural reserve; infrared thermography; tectonics; rockfalls



**Citation:** Pappalardo, G.; Mineo, S.; Carbone, S.; Monaco, C.; Catalano, D.; Signorello, G. Preliminary Recognition of Geohazards at the Natural Reserve “Lachea Islet and Cyclop Rocks” (Southern Italy). *Sustainability* **2021**, *13*, 1082. <https://doi.org/10.3390/su13031082>

Academic Editor: Pablo Peri  
Received: 29 December 2020  
Accepted: 18 January 2021  
Published: 21 January 2021

**Publisher’s Note:** MDPI stays neutral with regard to jurisdictional claims in published maps and institutional affiliations.



**Copyright:** © 2021 by the authors. Licensee MDPI, Basel, Switzerland. This article is an open access article distributed under the terms and conditions of the Creative Commons Attribution (CC BY) license (<https://creativecommons.org/licenses/by/4.0/>).

## 1. Introduction

A geohazard is generally defined as a geological source of danger, characterized by the potential to create problems for the development of a human environment and threats to the safety and well-being of people. Several types of geohazards can be identified worldwide, including marine and fluvial environments, whose occurrence proves the Earth’s continuous evolutionary process [1]. Their identification and study are the first steps for the management of a territory, as these can be characterized through scientific approaches and are amenable to probabilistic analysis. Furthermore, these are strongly linked to the physical environment and manageable through minimization of their consequences [2,3]. Often, geohazards occur rapidly and without warning signs; this underlines the importance of studying and monitoring the threatened areas for risk management purposes. Rockfalls, rapid, and damaging slope instability processes are considered among the most hazardous and fatal landslide types worldwide [4–7]. One of the rockfall predisposing

factors is the poor physical-mechanical attitude of rock masses, which is often enhanced by heavy rainfalls, weathering agents, earthquakes, or presence of close tectonic structures. It is known that the occurrence of fault lines controls the slope deformation and stability [8–12]. A recurrent goal of international scientific works on rockfalls is the integration between different methodologies for the slope characterization and monitoring, especially when the accessibility of the study area is poor. Several remote survey methodologies are employed for such purposes, such as aerial or satellite image analysis [13–16], laser scanning [17–20], and infrared thermography (IRT) [21–25]. In particular, the application of IRT to rock masses is relatively new, promising and quick scientific procedure that provides interesting results in terms of both morphological analysis and detection of rock fracturing, water circulation, and loose material, thanks to the distribution of the surface temperatures characterizing the different elements cropping out along the studied slope [11,21–25]. The combination of IRT with other survey approaches proved a scientifically interesting tool for the characterization of peculiar areas threatened by rockfalls. The available literature encourages the continuous experimentation of such a methodology [22,26].

In this frame, this paper presents a preliminary study aimed at recognizing the main geohazards that threatens the natural reserve “Lachea Islet and Cyclop Rocks” located along the coastal sector of Mt. Etna (Figure 1) in eastern Sicily (southern Italy). The natural reserve is represented by a small volcanic archipelago made up of an islet and widespread sea rocks (Figure 2), which is also mentioned by mythological stories whose existence is linked to the initial volcanic activity of Mount Etna, now part of the UNESCO World Heritage List. This study is focused on the rock mass condition found at the “Faraglione Grande” (FG), which is the greatest sea rock located south of Lachea Islet (Figures 1 and 2). Due to past and recent rockfall occurrences, the fruition of this area is subjected to restrictions, although crowds of tourist converge there especially during the summer. Moreover, data from the literature [27–32] reports the presence of a complex tectonic setting, with several fault segments crossing the area and belonging to regional active systems. The combination of these aspects highlights the need of specialist studies focused on the identification and characterization of the geohazards threatening the area in the perspective of planning risk mitigation measures. Nevertheless, the ground survey is not easy, and it should be preceded by the knowledge of preliminary information on the state of rock masses. In this paper, the survey of FG was carried out by remote methodologies through the combination of IRT and aerial photo analysis to recognize the potential unstable rock mass sectors and the evidence, if any, of tectonic structures. In particular, IRT was applied to map the variation of surface temperature affecting the framed rock mass, arising from the different elements occurring along it (e.g., bare or loose rock, vegetation), in order to recognize morphological features linked to instability processes. By combining IRT outcomes with morphological-aerial data, the likely unstable rock mass sectors were identified and rockfall trajectory simulations were carried out to establish a safety boundary around FG for its safe fruition. On the other hand, from a scientific point of view, IRT data were also compared to peculiar morphological features affecting FG, likely belonging to tectonic structures, in order to attempt an innovative data correlation with the structural setting of the area, thus paving the way to new IRT applications in geosciences.

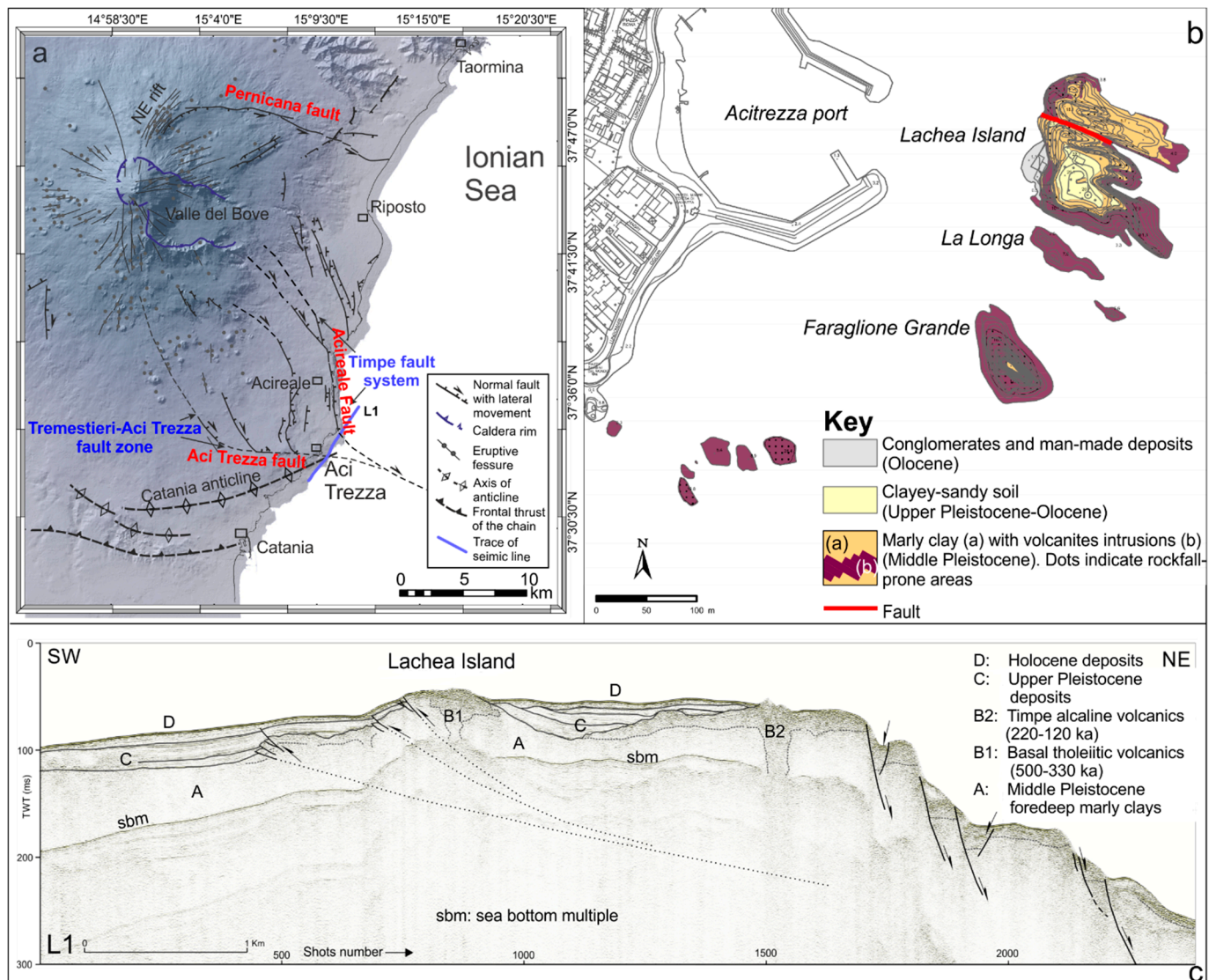


**Figure 1.** (a) Structural framework of the eastern and southern flanks of Mt. Etna (modified from [32]); (b) geological sketch of the natural reserve (data from CUTGANA archive); (c) Seismo-stratigraphic and tectonic interpretation of the high-resolution seismic profile L1 (see Figure 1a for location) showing contractional fold and thrust structures in the area of Lachea island and Cyclop Rocks (offshore prolongation of the Catania anticline) and extensional structures towards the northeast, where the Timpe normal fault system occurs (modified from [32]).





**Figure 2.** (a) overview on the Lachea Islet and Cyclop Rocks natural reserve (photo from CUTGANA archive); (b) Lachea Islet; (c) the main sea rock “Faraglione Grande” (FG).

## 2. The Natural Reserve “Lachea Islet and Cyclop Rocks”

About half a million years ago, a series of submarine eruptions gave rise to the early activity of Mt. Etna (Figure 1a), one of the most relevant active volcanoes in the world. It has been part of the UNESCO World Heritage List since 2013 thanks to its exceptional level of volcanic activity, which has been documented for over 2700 years. Its notoriety, scientific importance, and cultural-educational value are considered by UNESCO to have global significance. The first of the evolutionary phases of the volcano [33,34] mainly occurred in a submarine environment and led to the formation of a subvolcanic basaltic intrusion that was later tectonically uplifted and dismantled by sea waves, giving rise to a small archipelago of a small island (Lachea Islet) and a series of sea rocks (Cyclop Rocks or Faraglioni) (Figure 2a).

The basaltic rocks constituting the Lachea Islet and Cyclop Rocks are mainly represented by magmatic intrusions, pillow lava, and hyaloclastites, as well as tholeiitic volcanoclastites, interbedded within the middle-Pleistocene clayey succession, which is still visible on the top of both Lachea and the greatest rock (Faraglione Grande) (Figures 1b and 2b). From a petrographic point of view, rocks are characterized by a dark groundmass, with olivine, plagioclase phenocrysts, and femic minerals. Such composition plays an important role due to the high predisposition of weathering processes. From a larger scale point of view, rock masses are characterized by the typical, suggestive, and columnar aspects resulting from the slow cooling process of lava.

Some archaeological remains found on the islet testify to human presence dating back to prehistoric times, highlighting the relevance of this spot from a cultural heritage point of view. In 1998, the archipelago, along with the surrounding strip of sea, became a natural reserve, hosting a wide variety of flora and fauna. The Faraglione Grande (FG) or Santa Maria islet are the only sea rocks of the reserve to host a man-made manufacture, i.e., a stairway that leads to a small square where a religious statue is placed (Figure 2c). Nevertheless, due to the poor condition of the rock cliffs, the fruition of the island and Faraglioni rocks is subject to restrictions. In fact, mooring is forbidden in the proximity of the rocks and some paths, such as the one on FG, are closed to public. This is due to the progressive weathering of the rock mass that arise from meteoric agents (sea waters and wind) and enhanced by the fracturing of the rock itself. Moreover, signs of rock detachments are present along the cliff of the archipelago, thus representing a threat for the fruition of such public site.

### 3. Methodological Approach

This study is focused on the “Faraglione Grande” (FG), which is the greatest sea rock located south of the Lachea Islet (Figure 1), and aims to achieve a preliminary qualitative knowledge on the condition of the rock mass through the use of IRT as a remote survey methodology. This technique is based on the detection, acquisition, processing, and rendering of the thermal radiation, invisible to the human eye, emitted by an object throughout the infrared spectrum (wavelengths between 700 nm to 1 mm) [35]. The emission of such radiation is a property owned by any physical substance characterized by a higher temperature than the absolute zero, and it is directly proportional to the temperature itself. Therefore, IRT is widely employed to detect and represent, on a color-scaled image, the surface temperature of objects, structures, living organisms, and more [36]. The application of this technique to slope instability issues is still pioneering and some literature proves its utility in detecting the rock grade of fracturing, presence of water, and lithological variations based on the distribution of the detected surface temperature values [37–40]. With specific reference to rock mass, Pappalardo et al. [21,22] demonstrated that thermal images acquired in daylight conditions return information on the different orientation of rock mass portions, highlighting that hollow sectors keep lower surface temperatures than protruding ones due to the different solar irradiation. Similarly, abrupt variations of rock face orientation can be identified. According to such background and with the aim of mapping the surface temperature variation on the FG flank, in this study, an IRT acquisition campaign was carried out by choosing a stable shooting point on the Lachea Islet, which frames the FG northeastern side. In fact, due to the logistics of the area, the best viewpoint for the technical observation of the FG rock face is from sea and no direct rock mass survey can be performed without mandatory authorization. A high-sensitivity thermal camera (320 × 240 pixels infrared resolution) set in the range of temperature (20/650 °C (with ±2 °C accuracy)) was employed. Thermal images were processed via the software FLIR Tools to recognize the areas affected by different thermal outcomes in order to identify rock mass portions characterized by the presence of loose material, hollow morphology, bare rock, and vegetation. The most significant elements, referred to as both rockfalls and tectonic features, were highlighted on the images and compared to the elements directly observed by circumnavigating FG, thus leading to the recognition of the



most critical rock mass sectors. These are assumed as potential rockfall source areas, which were herein taken into account for the simulation of the rockfall trajectory. In fact, once assumed (and then verified) that the sea represents the receptor for falling boulders, the definition of a “safety distance” from FG would be useful for the nautical fruition of this part of the reserve. More specifically, rockfall simulations were carried out by considering 1 m<sup>3</sup> representative blocks, which is a reliable mean value estimated during the surveys. Trajectories were simulated according to the “Lumped Mass” method, which is based on a particle analysis [41] assuming that a falling rock is an infinitely small mass point affected by velocity reduction after a collision, with no influence of its shape and the size [42]. In particular, the steep slope topography was reconstructed on a 2D diagram with spatial coordinates for height and progressive distance. Along this section, the topography was assigned a couple of coefficients of restitution values [43] (i.e., 0.35 and 0.85 for normal and tangential coefficients, respectively) and blocks were “launched” from the height corresponding to the identified loose material. Starting from the average volume, a mass of 2700 kg was considered for the lumped mass application, according to the known physical properties of such rocks [44].

Finally, the morphological features corresponding to tectonic structures, highlighted by IRT, were compared to the available literature data on the structural setting of this area and validated by aerial photo evidence in order to provide an updated map of the local structural alignments.

#### 4. Geological Framework

At Mt. Etna, the earliest phase of discontinuous and scattered fissural volcanic activity, named Basal Tholeiitic [33,34,45,46], occurred about 500 ka and 330 ka ago in the foredeep basin at the front of the chain (e.g., in the Aci Trezza area). It caused the intrusion (Figure 1c) of the Aci Trezza laccolith in clayey sediments, whose remnants formed the Lachea islet and Cyclop Rocks. These are characterized by columnar jointing resulting from the cooling process of the lava body. At the top of Lachea islet and FG, whitish marly clays represent the remnant of the pre-existing Pleistocene clayey seafloor (Figure 1b). Other volcanic products emplaced between 220 and 120 ka ago (Timpe phase) reside along the Ionian coast north of the study area [33,34,45,46]. They are represented by plugs of columnar lavas and proximal pyroclastic deposits, cropping out at the bottom of the Acireale fault scarp (Figure 1a,c) [47]. In this time span, the extensional tectonics of the Ionian margin of Sicily [27,28,48] favored the alkaline magma ascent in the Mt. Etna region, turning the previous scattered fissural volcanism into a central activity that, about 100 ka ago, shifted westward to build the current volcanic edifice [27,33,34,45,46].

The lower eastern flank of Mt. Etna is characterized by several morphological scarps (locally known as Timpe), which are the result of late quaternary normal-oblique faulting (Timpe fault system) [27,28,47]. The Timpe fault system is considered responsible for the strong Upper Pleistocene–Holocene footwall uplift of the southeastern coastal sector of Mt. Etna [28]. In the same period, the foredeep clayey deposits and the overlying coastal-alluvial deposits, located along the volcano’s southern margin, have been involved in the compressive deformation at the front of the chain. GPS measurements over the last 20 years have revealed a shortening rate of ~5 mm/year along an NNW-SSE oriented axis of compression, which is consistent with the focal mechanism of deep earthquakes generated by the collisional front of the chain (see [49] and references therein). Interferometric data have highlighted the current growth of a large ~W-E oriented anticline in the northwestern outskirts of Catania [50], extending to the east as far as the Aci Trezza study area (the Catania anticline) [32,49] (Figure 1a). The Catania Anticline is characterized by maximum uplift rate of about 10 mm/year along the hinge zone and it has been interpreted as folding related to a shallow thrust migrating within the foredeep deposits at the chain front.

A high-resolution seismic investigation provided new insights on the geometry and activity of tectonic structures occurring in the offshore between Catania and Aci Trezza [32]. In particular, reflectors with divergent geometry suggest syn-tectonic deposition within

small growth folding basins (Figure 1c). This feature, together with reverse-mode displaced reflectors and folded seafloor, confirms that shortening has occurred offshore during the Late Pleistocene–Holocene in the Aci Trezza. It is worth noting that the Aci Trezza laccolith has been involved in contraction a long time after its intrusion, as suggested by seismic profiles acquired in the Aci Trezza offshore, clearly showing the Lachea island on the fold hinge [32]. Folding detected in the seismic sections can be easily correlated to the offshore extension of the large WSW–ENE trending Catania anticline, growing north of Catania city (Figure 1a), supported also by interferometric data [50]. In fact, radiometric dating of measured paleoshorelines occurring along the coastline between Catania and Aci Trezza [51] suggests an uplift-rate of about 3 mm/year in the last 4 ka at the fold hinge. Seismic profiles also show the offshore prolongation of the Timpe fault system (Figure 1c).

The general process of uplifting, related to volcano-tectonic regional processes [52] or to local deformation along faults and/or folds [49,51], is locally interrupted by subsidence related to flank sliding of the volcanic edifice. A literature review [28,53] indicated that the eastern flank of the Mt. Etna volcano has been sliding seaward. In particular, the sliding area is confined to the south by the WNW–ESE oriented right-lateral Tremestieri–Aci Trezza fault zone (Figure 1a), forcing the sliding to the east [54] and causing complex interactions with both the faults located along the coast [29,55] and the fold at the Aci Trezza offshore [32] (Figure 1c). The Lachea islet and adjacent rocks appear to be cut by several WNW–ESE faults and fractures (see below), which is probably related to the Aci Trezza fault activity. A fault segment clearly crops out at the Lachea Islet (Figure 1a). Some authors [29–31], mostly based on offshore data, assign great importance to this fault, inferring its continuation towards the Ionian abyssal plain.

## 5. Infrared Thermography Survey

The analysis of IRT images highlights a peculiar distribution of the surface temperatures along FG due to the daylight condition. By excluding the contribution of sky and sea, the best temperature range selected for the rock mass remote investigation is between 11 °C and 27 °C (Figure 3a). Such a range allows for the best-balanced definition of the mid-upper rock mass portion enclosed between the southeastern sun-radiated (highest surface temperatures) and the northwestern shadowed (lowest surface temperatures) FG flanks. In particular, a series of negative thermal anomalies outlines the presence of irregular and partly hollowed sectors that expose bare rock and facing northeast. These correspond to past rock detachment areas, where the sliding plane (SP) is still well exposed. Due to the columnar fracturing of the rock, typical of basalt formations, the failure might have been developed as a planar sliding along SP, involving single or multiple blocks. In particular, three main source areas can be identified on the IRT image (Figure 3a) as cold zones (surface temperature range 11.8–13 °C) surrounded by warmer sectors (surface temperature range 13–18 °C). The latter warm areas indicate the presence of protruding rock material, which can be assumed as loose rock locally hosting vegetation. This is well identifiable by constraining the surface temperature values in the range of 13–18 °C (Figure 3b). The most evident, even to the naked eye, vegetated spot is located on the top of FG, while some small bushes populate the openings between the basaltic columns, especially at the most weathered rock portions. Such areas were assumed herein as potential future rockfall source zones based on the thermal contrast with the bare rock sectors and on the visible match with loose rock material. The latter is represented by numerous blocks likely laying in a limit equilibrium condition on SP, thus constituting an element of hazard. It must be underlined that the typical basaltic columnar fracturing condition may enhance the release of blocks according to the most unfavorable kinematic failure mode.

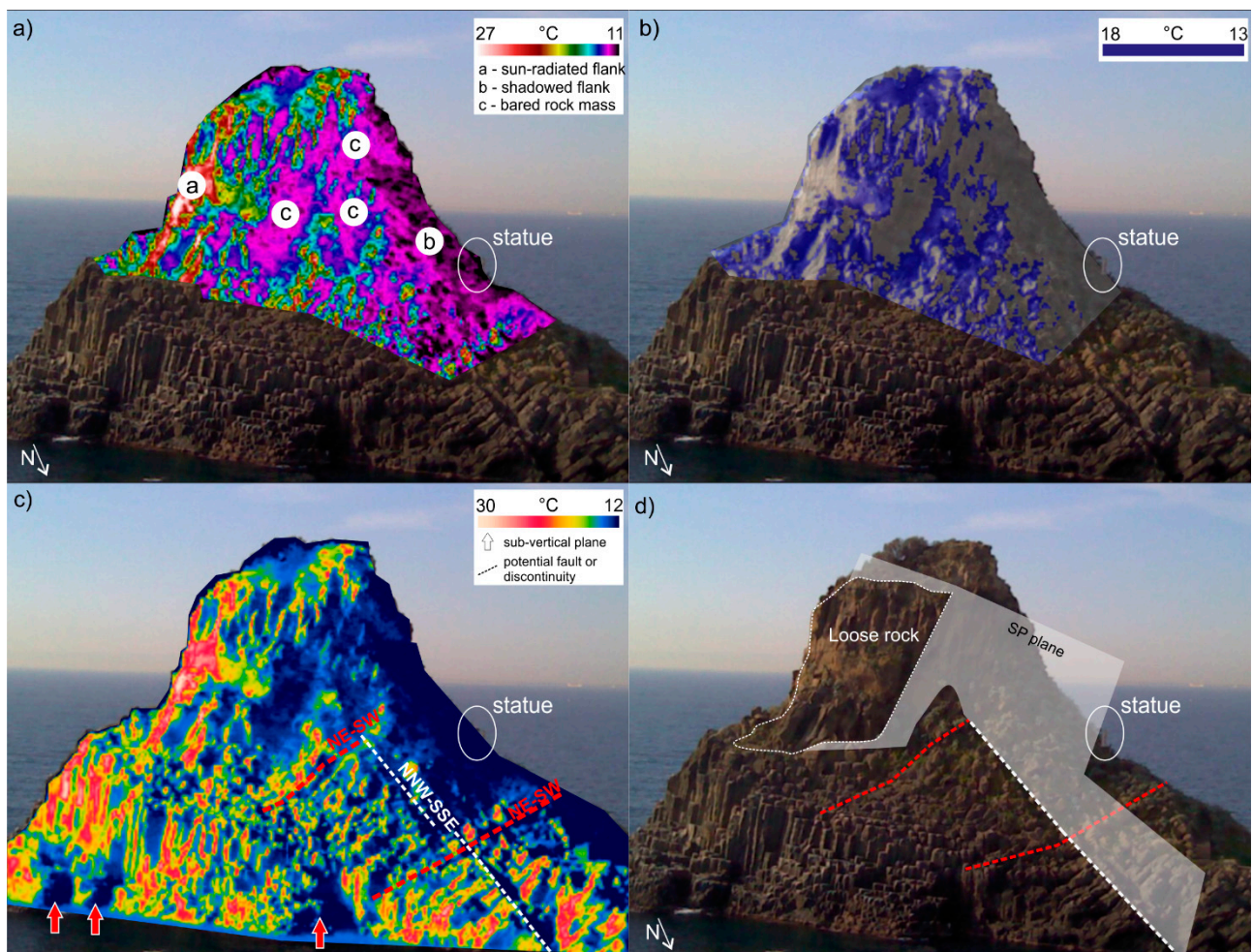


**Figure 3.** Infrared thermography (IRT) outcomes reported on a digital photo of Faraglione Grande (FG). (a) Range of surface temperature 27–11 °C; (b) temperature interval highlighted from 13 to 18 °C, labeling the warmer sectors surrounding the source areas; (c) main structural discontinuities (dashed white and red lines) recognized on the IRT image (arrows indicate the sub-vertical planes highlighted by negative thermal anomalies at the intersection with such discontinuities); (d) photointerpretation of IRT results.

By widening the range of selected temperatures, key considerations can be carried out even for the lower part of FG, where a linear, NNW-SSE trending, negative anomaly longitudinally crosses the sea rock (Figure 3c). This alignment, likely related to a structural discontinuity, is well highlighted in the IRT image as far as the rockfall source areas previously commented (Figure 3c). From a geometrical point of view, the above-mentioned daylighting failure plane SP seems to match with the structural plane belonging to such discontinuity, testifying the strong link between tectonics and rockfall occurrence (Figure 3d). Furthermore, two parallel ENE-WSW trending discontinuities cross FG and their morphological expression is well visible at the lowest portion of FG flank, where sub-vertical planes are highlighted by negative thermal anomalies at the intersection with such discontinuities (Figure 3c).

## 6. Rockfall Potential Trajectories

Once assessed, the predisposition to failure of the FG rock mass and the presence of hollow sectors suggests that the occurrence of past rockfalls did not block the deposition area. It is self-evident that the accumulation zone is located below the sea level due to the steepness of FG flanks, thus proving that the strip of sea surrounding FG is affected by



block transit. This represents a risk for both bathers (swimmers, canoeists, divers) and boats, especially during the summer, when tourists crowd the area.

In this perspective, starting from the location of the most evident loose blocks from both IRT survey (at the northeastern flank) and direct observation (at the south and southwestern flanks), potential rockfall trajectories were simulated along 2D profiles to preliminarily assess the width of the sea strip around FG affected by block transit. Simulations were carried out by considering 1000 trajectories along three representative sections of eastern, western, and southern flanks (Figure 4a). Achieved outcomes suggest that the fall of blocks is likely characterized by rebounds at the slope variation of the rock face, where kinetic energy ranges from 40 to 300 kJ (Figure 4b–d). The greatest energy values were found at the western section (Figure 4c) due to the steepness of the FG rock face. For the northern flank, a more detailed morphological survey is required to better define the most reliable sections for the definition of the potential trajectories. Nevertheless, due to the presence of unstable boulders laying along this flank, it is likely that blocks could reach and cross the stairway linking the docking spot to the Virgin statue, thus representing a key aspect to address for the ground fruition of this place.

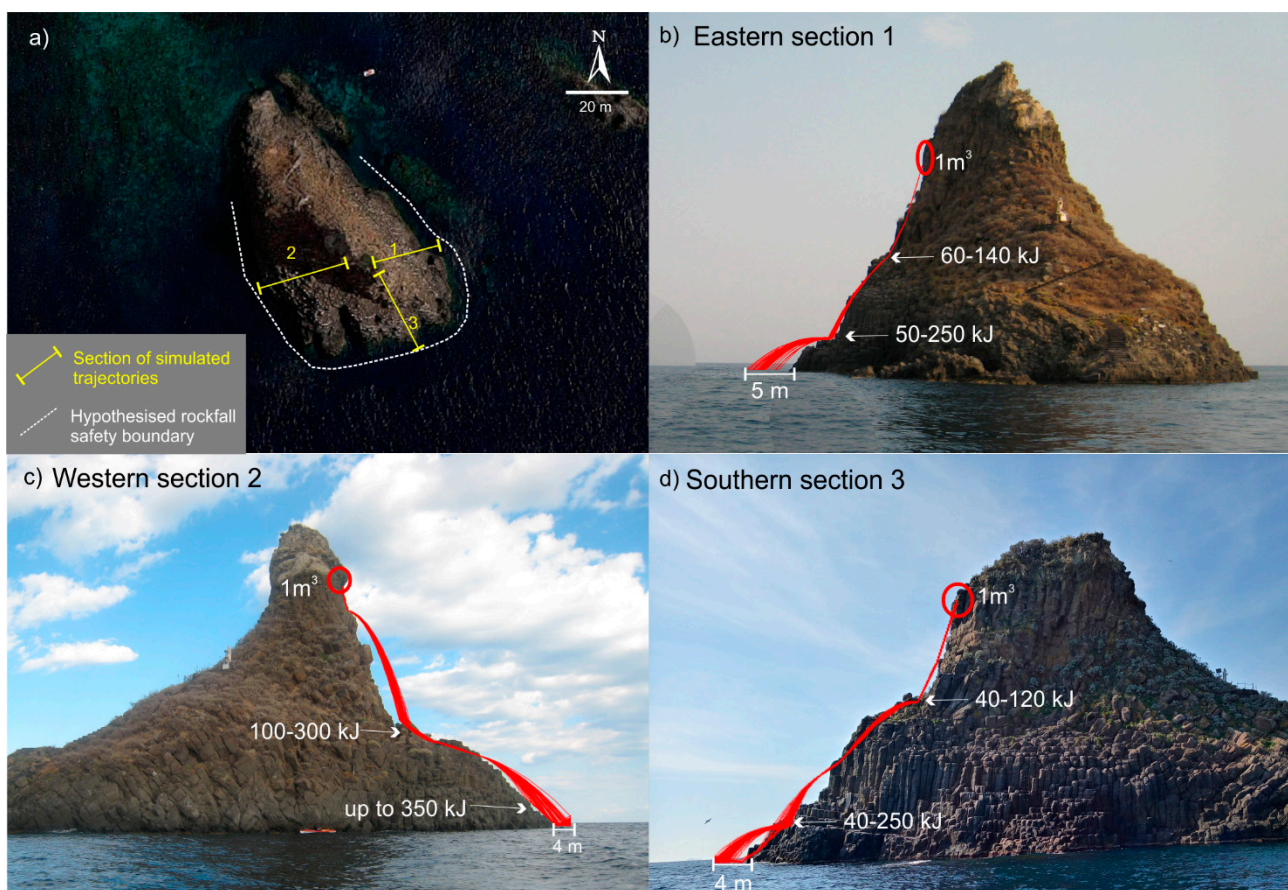


**Figure 4.** (a) Location of the rockfall trajectory simulation sections and resulting safety boundary around FG; (b) simulation at the east flank; (c) simulation at the west flank; (d) simulation at the south flank.

With the aim of defining a preliminary safety boundary around FG, the block running out points on the sea floor were taken into account. These are found within a distance from the rock mass ranging between 4 and 5 m (Figure 4), according to the simulated volumes, thus providing a useful hint for the maritime fruition planning of this strip of sea.

## 7. Discussion

Outcomes achieved by this preliminary study can be commented and discussed according to two main aspects: (1) the methodological approach, consisting of the innovative and pioneering integration between IRT surveys, and the morphological-aerial evidence of specific elements referred to as both rock slope instability and tectonics; (2) the scientific outcomes achieved by the study.

The methodological approach involving IRT confirmed the usefulness of such techniques applied to the rock mass characterization from a stability perspective, as already demonstrated in the literature in different geological and morphological frameworks [21–26]. In fact, IRT allows for the detection of specific rock mass features or anomalies based on the distribution of the surface temperature along the slope. It has been experienced that for surveys carried out in daylight, hints on the morphology of the rock mass can be gained by processing IRT images. This activity requires the selection of the most ideal temperature range in order to exclude the contribution of extreme temperature values, in this case related to sky and sea. Nevertheless, a certain grade of disturbance by the forced directional condition arising from the sun-radiation must be taken into account, which depends on the survey time and season. This is a limitation of the IRT survey daylight setting, which does not allow for a detailed analysis of shadowed and sun-facing rock mass sectors. On the other hand, a merit of this methodology is found in the possibility of performing quick surveys of wide areas, particularly useful when the accessibility is not feasible. Moreover, IRT outcomes can be easily integrated with morphological evidence arising from both ground and aerial surveys, such as the strong match between the tectonic evidence highlighted in this study. This is a novelty in the use of IRT for the rock mass survey, which strengthens the applicability of IRT in wide fields of geosciences. Pappalardo et al. [26] sensed the potential of IRT in mapping tectonic features, as they found a tectonic contact between two different geological formations. This was highlighted in a landslide area thanks to the thermal contrast between the two lithologies. In the case of FG, the tectonic lines cross the same geological unit and thus their presence is supported by morphological evidence producing thermal contrasts in the IRT images. Such a match was found in the analyzed thermograms, which allowed us to link the weakening action played by tectonics on rock masses to the related instability. In fact, the source areas of past rockfalls, identified by IRT, exposed a dip-slope plane, which was assumed as the rockfall sliding plane. Its orientation matched the NNW-SSE segment detected by IRT, thus suggesting the likely tectonic nature of such plane and corroborating the strong link between rockfalls and tectonics.

Based on this outcome, further results can be discussed in the frame of the local regional structural setting. In fact, the NNW-SSE segment recognized by IRT and reported in Figure 5b is parallel to an alignment morphologically marked by the presence of an inlet at the southern portion of FG, thus suggesting the presence of multiple segments in a close area. To the northeast, further segments can also be recognized by aerial photos of glimpsed submarine rocks, which are aligned along a preferential NW-SE direction (Figure 5b). These structures, together with the tectonic segments already described between the FG and Lachea islet, belong to the offshore extension of the Tremestieri-Aci Trezza fault zone. Moreover, an ENE-WSW set of discontinuities, whose IRT evidence is marked by two subvertical bare planes, was recognized at the FG. These structures could be related to extensional fracturing at the extrados of the fold deforming the crust under the Lachea islet and Cyclop Rocks (Figures 1c and 5b).



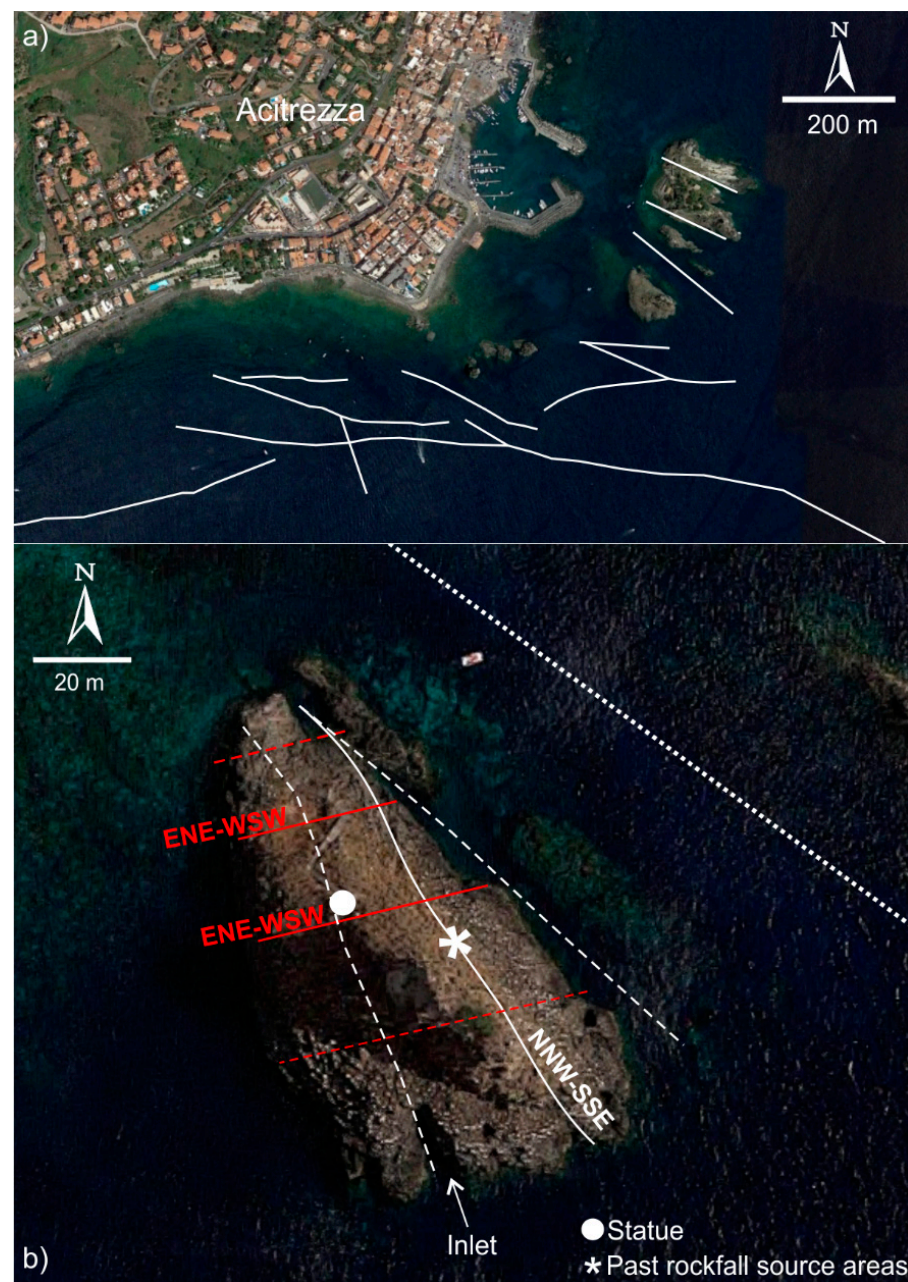


**Figure 5.** (a) Scheme of the main tectonic alignments (white lines) crossing the natural reserve (modified from [56]). Dashed rectangle encloses the inset b area; (b) discontinuity traces by IRT at FG and morphological evidence (dashed lines are alignments recognized from morphological evidence; continuous lines are alignments recognized by IRT; dotted line is a fault already mapped in inset a).

Finally, the identification of loose rock mass portions suggests the real possibility of future rockfalls threatening the fruition of this spot of the reserve. The rock properties are likely weakened by the weathering action of sea water and meteoric agents; in fact, due to its location, FG is well exposed to wind erosive mechanisms. Moreover, the columnar jointing of the rock mass is a further element enhancing the slope instability that should be taken into account for future in-depth studies. In fact, according to the spatial relationship between the orientation of both the slope face and the joints, single or multiple blocks can be released according to either sliding or toppling kinematics, giving rise to hazardous rockfalls affecting a strip of sea around FG that should be forbidden.



## 8. Conclusions

In this paper, we presented a preliminary recognition of geohazards at the natural reserve “Lachea Islet and Cyclop Rocks” in eastern Sicily by integrating IRT surveys and morphological-aerial interpretation. The study area fell in an active tectonic region where different fault systems characterized the landscape’s morphodynamical evolution. The natural reserve was instituted to protect and preserve a small volcanic archipelago that represented the early products of Mt. Etna. Due to the wide variety of flora, fauna, and landscape beauty, this area has long been a popular international tourist attraction, especially in the summertime. Nevertheless, the fruition of the Lachea islet and Faraglioni rocks has been subject to restrictions due to the poor condition of rock masses. The survey targeted for this study was the Faraglione Grande (FG), which is the greatest rock cliff of the archipelago that has suffered from past rockfalls. This was highlighted by the use of IRT to map the different surface temperatures along the rock mass. Thermal results highlighted the presence of hollow rock mass sectors exposing a bare sliding plane, corresponding to past detachment zones. These are surrounded by warmer sectors representing loose rock material, likely prone to future instability. Based on the comparison between IRT outcomes and aerial-morphological data interpretation, confirming the presence of loose rock materials at the highest sectors of FG, rockfall trajectory simulations demonstrated what was already conceivable, i.e., that the sea is the receptor for the totality of falling blocks from the simulated sections. This suggests the necessity of defining a 4–5 m wide safety boundary around FG in order to reduce the risk for boats, divers, and bathers, as well as to enhance the fruition of this tourist spot.

Since the NNW-SSE sliding planes and the ENE-WSW discontinuities match well with regional structural alignments, achieved outcomes testify the strong interaction between landslides and tectonics. In addition to these, the peculiar columnar fracturing characterizing volcanic rock masses can locally enhance the release of blocks failing according to the spatial orientation between rock faces and joints.

Finally, from a broader scientific perspective, the achieved results demonstrate the reliability of IRT as it was applied to the study of peculiar morpho-structural features and its potential in detecting tectonic structures signs, thus laying the foundations for further in-depth studies focused on new IRT application in the geosciences.

**Author Contributions:** Conceptualization and methodology: G.P., S.M., S.C., C.M.; supervision G.P., S.M., C.M.; field investigation: G.P., S.M.; geosite: S.C., G.S., D.C.; InfraRed Thermography: S.M., G.P.; structural setting: C.M.; writing and review S.M., G.P., C.M., S.C. All authors have read and agreed to the published version of the manuscript.

**Funding:** This research was financially supported by the “CH2V—Cultural Heritage Hazard and Vulnerability” project (Giovanna Pappalardo).

**Acknowledgments:** Thermal images were processed in the “Geologia Applicata” laboratory at the Department of Biological, Geological, and Environmental Sciences of Catania University. The authors would like to thank LAND (Laboratorio Analisi Non Distruttive) of the same department for lending the thermal camera.

**Conflicts of Interest:** The authors declare no conflict of interest.

## References

1. Culshaw, C.M. Geohazards. In *Encyclopedia of Engineering Geology. Encyclopedia of Earth Sciences Series*; Bobrowsky, P., Marker, B., Eds.; Available online: <https://link.springer.com/referencework/10.1007/978-3-319-73568-9> (accessed on 5 January 2021).
2. Keller, E.A.; Blodgett, R.H. *Natural Hazards: Earth's Processes as Hazards, Disasters, and Catastrophes*; Pearson Education, Inc.: Upper Saddle River, NJ, USA, 2006; p. 395.
3. Capps, D.; Anderson, D.A.; McKinley, M. Geohazard risk reduction along the Denali National Park Road. *Alsk. Park Sci.* **2019**, *18*, 44–51.
4. Guzzetti, F.; Stark, C.P.; Salvati, P. Evaluation of flood and landslide risk to the population of Italy. *Environ. Manag.* **2005**, *36*, 15–36. [[CrossRef](#)]

5. Palma, B.; Parise, M.; Reichenbach, P.; Guzzetti, F. Rock-fall hazard assessment along a road in the Sorrento Peninsula, Campania, southern Italy. *Nat. Hazards* **2012**, *61*, 187–201. [[CrossRef](#)]
6. Schweigl, J.; Ferretti, C.; Nössing, L. Geotechnical characterization and rockfall simulation of a slope: A practical case study from South Tyrol (Italy). *Eng. Geol.* **2003**, *67*, 281–296. [[CrossRef](#)]
7. De Vallejo, L.I.G.; Hernández-Gutiérrez, L.E.; Miranda, A.; Ferrer, M. Rockfall hazard assessment in volcanic regions based on ISVS and IRVS geomechanical indices. *Geosciences* **2020**, *10*, 220. [[CrossRef](#)]
8. Willenberg, H.; Loew, S.; Eberhardt, E.; Evans, K.; Spillmann, T.; Heincke, B.; Maurer, H.R.; Green, A. Internal structure and deformation of an unstable crystalline rock mass above Randa (Switzerland): Part I—Internal structure from integrated geological and geophysical investigations. *Eng. Geol.* **2008**, *101*, 1–14. [[CrossRef](#)]
9. Tokiwa, T.; Tsusaka, K.; Ishii, E.; Sanada, H.; Tominaga, E.; Hatsuyama, Y.; Funaki, H. Influence of a fault system on rockmass response to shaft excavation in soft sedimentary rock, Horonobe area, northern Japan. *Int. J. Rock Mech. Min. Sci.* **2011**, *48*, 773–781. [[CrossRef](#)]
10. Pappalardo, G.; Mineo, S.; Rapisarda, F. Rockfall hazard assessment along a road on the Peloritani Mountains (northeastern Sicily, Italy). *Nat. Hazards Earth Syst. Sci.* **2014**, *14*, 2735–2748. [[CrossRef](#)]
11. Mineo, S.; Pappalardo, G.; Rapisarda, F.; Cubito, A.; Di Maria, G. Integrated geostructural, seismic and infrared thermography surveys for the study of an unstable rock slope in the Peloritani Chain (NE Sicily). *Eng. Geol.* **2015**, *195*, 225–235. [[CrossRef](#)]
12. Pappalardo, G.; Imposa, S.; Barbano, M.S.; Grassi, S.; Mineo, S. Study of landslides at the archaeological site of Abakainon necropolis (NE Sicily) by geomorphological and geophysical investigations. *Landslides* **2018**, *15*, 1279–1297. [[CrossRef](#)]
13. Guerriero, L.; Di Martire, D.; Calcaterra, D.; Francioni, M. Digital image correlation of Google Earth images for Earth's surface displacement estimation. *Remote Sens.* **2020**, *12*, 3518. [[CrossRef](#)]
14. Solari, P.L.; Matteo, D.S.; Raspini, F.; Barra, A.; Bianchini, S.; Confuorto, P.; Casagli, N.; Crosetto, M. Review of satellite interferometry for landslide detection in Italy. *Remote Sens.* **2020**, *12*, 1351. [[CrossRef](#)]
15. Rodriguez, J.; Macciotta, R.; Hendry, M.T.; Roustaei, M.; Gräpel, C.; Skirrow, R. UAVs for monitoring, investigation, and mitigation design of a rock slope with multiple failure mechanisms—A case study. *Landslides* **2020**, *17*, 2027–2040. [[CrossRef](#)]
16. Deane, E.; Macciotta, R.; Hendry, M.T.; Gräpel, C.; Skirrow, R. Leveraging historical aerial photographs and digital photogrammetry techniques for landslide investigation—A practical perspective. *Landslides* **2020**, *17*, 1989–1996. [[CrossRef](#)]
17. Jaboyedoff, M.; Demers, D.; Locat, J.; Locat, A.; Locat, P.; Oppikofer, T.; Robitaille, D.; Turmel, D. Use of terrestrial laser scanning for the characterization of retrogressive landslides in sensitive clay and rotational landslides in river banks. *Can. Geotech. J.* **2009**, *46*, 1379–1390. [[CrossRef](#)]
18. Fanti, R.; Gigli, G.; Lombardi, L.; Tapete, D.; Canuti, P. Terrestrial laser scanning for rockfall stability analysis in the cultural heritage site of Pitigliano (Italy). *Landslides* **2012**, *10*, 409–420. [[CrossRef](#)]
19. Gordon, S.; Lichti, D.; Stewart, M. Application of high-resolution, ground based laser scanner for deformation measurements. In Proceedings of the 10th International FIG Symposium on Deformation Measurements, Orange, CA, USA, 19–22 March 2001; pp. 23–32.
20. Mineo, S.; Pappalardo, G.; Mangiameli, M.; Campolo, S.; Mussumeci, G. Rockfall analysis for preliminary hazard assessment of the cliff of Taormina Saracen Castle (Sicily). *Sustainability* **2018**, *10*, 417. [[CrossRef](#)]
21. Pappalardo, G.; Mineo, S.; Zampelli, S.P.; Cubito, A.; Calcaterra, D. InfraRed thermography proposed for the estimation of the cooling Rate Index in the remote survey of rock masses. *Int. J. Rock Mech. Min. Sci.* **2016**, *83*, 182–196. [[CrossRef](#)]
22. Pappalardo, G.; Mineo, S.; Imposa, S.; Grassi, S.; Leotta, A.; La Rosa, F.; Salerno, D. A quick combined approach for the characterization of a cliff during a post-rockfall emergency. *Landslides* **2020**, *17*, 1063–1081. [[CrossRef](#)]
23. Frodella, W.; Gigli, G.; Morelli, S.; Lombardi, L.; Casagli, N. Landslide mapping and characterization through infrared thermography (IRT): Suggestions for a methodological approach from some case studies. *Remote Sens.* **2017**, *9*, 1281. [[CrossRef](#)]
24. Gigli, G.; Morelli, S.; Fornera, S.; Casagli, N. Terrestrial laser scanner and geomechanical surveys for the rapid evaluation of rock fall susceptibility scenarios. *Landslides* **2012**, *11*, 1–14. [[CrossRef](#)]
25. Casagli, N.; Frodella, W.; Morelli, S.; Tofani, V.; Ciampalini, A.; Intrieri, E.; Raspini, F.; Rossi, G.; Tanteri, L.; Lu, P. Spaceborne, UAV and ground-based remote sensing techniques for landslide mapping, monitoring and early warning. *Geoenvirom. Disasters* **2017**, *4*, 9. [[CrossRef](#)]
26. Pappalardo, G.; Mineo, S.; Angrisani, A.C.; Di Martire, D.; Calcaterra, D. Combining field data with infrared thermography and DInSAR surveys to evaluate the activity of landslides: The case study of Randazzo Landslide (NE Sicily). *Landslides* **2018**, *15*, 2173–2193. [[CrossRef](#)]
27. Monaco, C.; De Guidi, G.; Ferlito, C. The Morphotectonic map of Mt. Etna. *Ital. J. Geosci.* **2010**, *129*, 408–428.
28. Azzaro, R.; Bonforte, A.; Branca, S.; Guglielmino, F. Geometry and kinematics of the fault systems controlling the unstable flank of Etna volcano (Sicily). *J. Volcanol. Geotherm. Res.* **2013**, *251*, 5–15. [[CrossRef](#)]
29. Gross, F.; Krastel, S.; Geersen, J.; Behrmann, J.H.; Ridente, D.; Chiocci, F.L.; Bialas, J.; Papenberg, C.; Cukur, D.; Urlaub, M.; et al. The limits of seaward spreading and slope instability at the continental margin offshore Mt Etna, imaged by high-resolution 2D seismic data. *Tectonophysics* **2016**, *667*, 63–76. [[CrossRef](#)]
30. Gutscher, M.-A.; Dominguez, S.; Lépinay, B.M.; Pinheiro, L.; Gallais, F.; Babonneau, N.; Cattaneo, A.; Le Faou, Y.; Barreca, G.; Micallef, A.; et al. Tectonic expression of an active slab tear from high-resolution seismic and bathymetric data offshore Sicily (Ionian Sea). *Tectonics* **2016**, *35*, 39–54. [[CrossRef](#)]

31. Carlino, M.F.; Cavallaro, D.; Coltelli, M.; Cocchi, L.; Zgur, F.; Patanè, D. Time and space scattered volcanism of Mt. Etna driven by strike-slip tectonics. *Sci. Rep.* **2019**, *9*, 12125. [[CrossRef](#)]
32. Barreca, G.; Corradino, M.; Monaco, C.; Pepe, F. Active tectonics along the south east offshore margin of Mt. Etna: New insights from high-resolution seismic profiles. *Geosciences* **2018**, *8*, 62. [[CrossRef](#)]
33. Tanguy, J.-C.; Condomines, M.; Kieffer, G. Evolution of the Mount Etna magma: Constraints on the present feeding system and eruptive mechanism. *J. Volcanol. Geotherm. Res.* **1997**, *75*, 221–250. [[CrossRef](#)]
34. Gillot, P.Y.; Kieffer, G.; Romano, R. The evolution of Mount Etna in the light of potassium-argon dating. *Acta Vulcanol.* **1994**, *5*, 81–87.
35. Hillel, D. *Environmental Soil Physics*; Academic Press: San Diego, CA, USA, 1998; p. 771.
36. Ammer, K. Thermography 2015—A computer-assisted literature survey. *Thermol. Int.* **2016**, *26*, 5–42.
37. Wu, J.-H.; Lin, H.-M.; Lee, D.-H.; Fang, S.-C. Integrity assessment of rock mass behind the shotcreted slope using thermography. *Eng. Geol.* **2005**, *80*, 164–173. [[CrossRef](#)]
38. Baroň, I.; Bečkovský, D.; Miča, L. Application of infrared thermography for mapping open fractures in deep-seated rockslides and unstable cliffs. *Landslides* **2012**, *11*, 15–27. [[CrossRef](#)]
39. Mineo, S.; Calcaterra, D.; Zampelli, S.P.; Pappalardo, G. Application of infrared thermography for the survey of intensely jointed rock slopes. *Rend. Online Soc. Geol. Ital.* **2015**, *35*, 212–215. [[CrossRef](#)]
40. Pappalardo, G.; Mineo, S. Study of jointed and weathered rock slopes through the innovative approach of InfraRed thermography. In *Advances in Natural and Technological Hazards Research*; Springer Nature: Cham, Switzerland, 2018; Volume 50, pp. 85–103.
41. Hoek, E. *RockFall—A Program for the Analysis of Rockfalls from Slopes*; Department of Civil Engineering, University of Toronto: Toronto, ON, Canada, 1987.
42. Ku, C.-Y. Modeling of rockfalls using the lumped mass method and DDA. In *Rock Characterization, Modeling and Engineering Design Methods*; Feng, X.-F., Hudson, J.A., Tan, F., Eds.; CRC Press: London, UK, 2013; pp. 469–474.
43. Pfeiffer, T.J.; Bowen, T.D. Computer simulation of rockfalls. *Environ. Eng. Geosci.* **1989**, *26*, 135–146. [[CrossRef](#)]
44. Pappalardo, G.; Mineo, S. Investigation on the mechanical attitude of basaltic rocks from Mount Etna through InfraRed thermography and laboratory tests. *Constr. Build. Mater.* **2017**, *134*, 228–235. [[CrossRef](#)]
45. De Beni, E.; Branca, S.; Coltelli, M.; Groppelli, G.; Wijbrans, J. <sup>39</sup>Ar/<sup>40</sup>Ar isotopic dating of Etna volcanic succession. *Ital. J. Geosci.* **2011**, *130*, 292–305. [[CrossRef](#)]
46. Branca, S.; Coltelli, M.; De Beni, E.; Wijbrans, J. Geological evolution of Mount Etna volcano (Italy) from earliest products until the first central volcanism (between 500 and 100 ka ago) inferred from geochronological and stratigraphic data. *Acta Diabetol.* **2007**, *97*, 135–152. [[CrossRef](#)]
47. Corsaro, R.A.; Neri, M.; Pompilio, M. Paleo-environmental and volcano-tectonic evolution of the southeastern flank of Mt. Etna during the last 225 ka inferred from the volcanic succession of the ‘Timpe’, Acireale, Sicily. *J. Volcanol. Geotherm. Res.* **2002**, *113*, 289–306. [[CrossRef](#)]
48. Monaco, C.; Tapponnier, P.; Tortorici, L.; Gillot, P. Late Quaternary slip rates on the Acireale-Piedimonte normal faults and tectonic origin of Mt. Etna (Sicily). *Earth Planet. Sci. Lett.* **1997**, *147*, 125–139. [[CrossRef](#)]
49. De Guidi, G.; Barberi, G.; Barreca, G.; Bruno, V.; Cultrera, F.; Grassi, S.; Imposa, S.; Mattia, M.; Monaco, C.; Scarfi, L.; et al. Geological, seismological and geodetic evidence of active thrusting and folding south of Mt. Etna (eastern Sicily): Reevaluation of “seismic efficiency” of the Sicilian basal thrust. *J. Geodyn.* **2015**, *90*, 32–41. [[CrossRef](#)]
50. Bonforte, A.; Guglielmino, F.; Coltelli, M.; Ferretti, A.; Puglisi, G. Structural assessment of Mount Etna volcano from Permanent Scatterers analysis. *Geochem. Geophys. Geosystems* **2011**, *12*, 12. [[CrossRef](#)]
51. Branca, S.; De Guidi, G.; Lanzafame, G.; Monaco, C. Holocene vertical deformation along the coastal sector of Mt. Etna volcano (eastern Sicily, Italy): Implications on the time–space constrains of the volcano lateral sliding. *J. Geodyn.* **2014**, *82*, 194–203. [[CrossRef](#)]
52. De Guidi, G.; Imposa, S.; Scudero, S.; Palano, M. New evidence for late Quaternary deformation of the substratum of Mt. Etna volcano (Sicily, Italy): Clues indicate active crustal doming. *Bull. Volcanol.* **2014**, *76*, 1–13. [[CrossRef](#)]
53. Mattia, M.; Bruno, V.; Caltabiano, T.; Cannata, A.; Cannavò, F.; D’Alessandro, W.; Di Grazia, G.; Federico, C.; Giammanco, S.; La Spina, A.; et al. A comprehensive interpretative model of slow slip events on Mt. Etna’s eastern flank. *Geochem. Geophys. Geosystems* **2015**, *16*, 635–658. [[CrossRef](#)]
54. De Guidi, G.; Brighenti, F.; Carnemolla, F.; Imposa, S.; Marchese, S.A.; Palano, M.; Scudero, S.; Vecchio, A. The unstable eastern flank of Mt. Etna volcano (Italy): First results of a GNSS-based network at its southeastern edge. *J. Volcanol. Geotherm. Res.* **2018**, *357*, 418–424. [[CrossRef](#)]
55. Chiocci, F.L.; Coltelli, M.; Bosman, A.; Cavallaro, D. Continental margin large-scale instability controlling the flank sliding of Etna volcano. *Earth Planet. Sci. Lett.* **2011**, *305*, 57–64. [[CrossRef](#)]
56. Cavallaro, D.S. *Indagini Geologiche Integrate (Terra-Mare) del Bordo Orientale Emerso e Sommerso del M. Etna e Relazioni con L’evoluzione Geodinamica dell’Area*. Ph.D. Thesis, Università di Catania, Catania, Italy, 2010.